Altering the Balance between Ligand-Based Radical Anion Formation and Dechelation in Electrochemically Reduced Binuclear Copper(I) Complexes: A Resonance Raman Spectroelectrochemical Study

Simon E. Page and Keith C. Gordon*,†

Department of Chemistry, University of Otago, P.O. Box 56, Dunedin, New Zealand

Anthony K. Burrell*

Department of Chemistry, Massey University, Private Bag 11122, Palmerston North, New Zealand

Received December 2, 1997

The electrochemistry and spectral properties of a series of mono- and binuclear complexes with bridging ligands based on 2,3-di(2-quinolyl)quinoxaline are reported. The ligands are 2,3-di(2-quinolyl)quinoxaline (dqq), 6,7-dimethyl-2,3-di(2-quinolyl)quinoxaline ($dqqMe_2$), and 6,7-dichloro-2,3-di(2-quinolyl)quinoxaline ($dqqCl_2$). The complexes are $[Cu(dqq)(PPh_3)_2]BF_4$, **1**·$[BF_4]$; $[Cu(dqqMe_2)(PPh_3)_2]BF_4$, **2**·$[BF_4]$; $[Cu(dqqCl_2)(PPh_3)_2]BF_4$, **3**·$[BF_4]$; $[(PPh_3)_2Cu(dqq)Cu(PPh_3)_2](BF_4)_2$, **4**·$[BF_4]_2$; $[(PPh_3)_2Cu(dqqMe_2)Cu(PPh_3)_2](BF_4)_2$, **5**·$[BF_4]_2$; $[(PPh_3)_2Cu(dqqCl_2)$-$Cu(PPh_3)_2](BF_4)_2$, **6**·$[BF_4]_2$. The mononuclear complexes reduce at the metal and dechelate, as evidenced by UV/vis spectroelectrochemistry. Reduction of the binuclear complexes results in ligand-based radical anion formation for **4** and **6** but decomposition of **5** to **2**. The reduction species are identified using resonance Raman spectroscopy. The structures of $[Cu(PPh_3)_2(C_{26}H_{14}Cl_2N_4)][BF_4]$ (**3**·$[BF_4]$) and $[(Cu(PPh_3)_2)_2(C_{26}H_{14}Cl_2N_4)][BF_4]_2$·$2CH_2$-$Cl_2$ (**6**·$[BF_4]_2$) were determined by single-crystal X-ray diffraction. **3**·$[BF_4]$ crystallized in the monoclinic space group $P\bar{1}$ with cell dimensions $a = 10.956(2)$ Å, $b = 15.278(3)$ Å, $c = 16.032(3)$ Å, $\alpha = 100.342(8)°$, $\beta = 95.291(13)°$, $\gamma = 93.968(12)°$, $Z = 2$, $\rho_{calcd} = 1.431$ g/cm^3, and $R(F_o) = 0.0589$. **6**·$[BF_4]_2$ crystallized in the monoclinic space group $C2/c$ with cell dimensions $a = 21.295(4)$ Å, $b = 24.322(5)$ Å, $c = 20.034(4)$ Å, $\beta = 112.64(3)°$, $Z = 8$, $\rho_{calcd} = 1.486$ g/cm^3, and $R(F_o) = 0.0422$.

Introduction

We are interested in the behavior of copper(I) complexes with polypyridyl ligands that may bridge metal centers. Our stimulus for these studies comes from the use of copper(I) polypyridyl complexes in the construction of supramolecular assemblies.[1] These may be used in solar energy harvesting systems. The utility of an assembly constructed from copper(I) polypyridyl units, with regard to solar energy applications, lies in the multichromophoric nature of the system coupled with the ability to transduce energy along the assembly. This is well established in ruthenium(II) and rhenium(I) polynuclear complexes.[2] Recently a number of copper(I) complexes have been studied that also undergo energy transduction and charge-separation.[3] If copper(I) systems are to be used for such applications then it is critically important to understand how the building blocks of the assembly behave with respect to electron transfer. Very little is known about the behavior of copper(I) complexes with bridging ligands in regard to electrochemical reduction.[4] In many copper(I) complexes reduction leads to dechelation of the complex.[5]

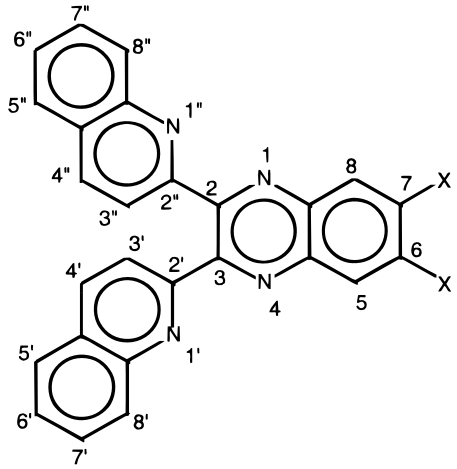

Figure 1. Ligands and numbering system used.

The bridging ligands used in this study are based on 2,3-di-(2-quinolyl)quinoxaline (dqq), and the extensive π conjugation of these ligands makes them good electron acceptors. The ligands are shown in Figure 1.

We have investigated a series of mono- and binuclear complexes with the $[Cu(PPh_3)_2]^+$ moiety. This is a particularly

* Corresponding authors.
† E-mail address: kgordon@alkali.otago.ac.nz.

(1) (a) Baxter, P.; Lehn, J.-M.; DeCain, A.; Fischer, J. *Angew. Chem., Int. Ed. Engl.*, **1993**, *32*, 69. (b) Marquis-Rigault, A.; Dupont-Gervais, A.; Van Dorsselaer, A.; Lehn, J.-M. *Chem. Eur. J.* **1996**, *2*, 1395. (c) Lehn, J.-M.; Rigault, A.; Siegel, J.; Harrowfield, J.; Chevrier, B.; Moras, D. *Proc. Natl. Acad. Sci. U.S.A.* **1987**, *84*, 2565. (d) Lehn, J.-M.; Rigault, A. *Angew. Chem., Int. Ed. Engl.* **1988**, *27*, 1095. (e) Lehn, J.-M.; Harding, M. M.; Koert, U.; Marquis-Rigault, A.; Piguet, C.; Siegel, J. *Helv. Chim. Acta* **1991**, *74*, 594. (f) Lehn, J.-M. *Supramolecular Chemistry*; VCH: Weinheim, 1995; Chapter 9.
(2) Balzani, V.; Juris, A.; Venturi, M.; Campagna, S.; Serroni, S. *Chem. Rev.* **1996**, *96*, 759.
(3) Ruthkosky, M.; Kelly, C. A.; Zaros, M. C.; Meyer, G. J. *J. Am. Chem. Soc.* **1997**, *119*, 12004 and references therein.
(4) Kohlman, S.; Kaim, W. *Inorg. Chem.* **1987**, *26*, 1469.
(5) Sauvage, J.-P. *J. Am. Chem. Soc.* **1988**, *111*, 7791.

S0020-1669(97)01505-X CCC: $15.00
Published on Web 08/07/1998

useful species to use in spectroscopic studies because the PPh_3 ligands do not possess chromophores in the visible region which greatly simplifies spectral interpretation.[6]

The crystal structures for a mononuclear and its corresponding binuclear complex are presented. These show the structural differences resulting from addition of the second metal center. These changes may be related to the electrochemical properties. It is also possible to compare the structural differences between the reported dqq ligands and complexes with the previously studied dpq-based ligands (dpq is 2,3-di(2-pyridyl)quinoxaline). We find that all of the mononuclear complexes dechelate when reduced. For the binuclear complexes dechelation or reduction of the ligand may occur depending on the substituents of the ligand. These properties are very surprising in view of the low reduction potentials for the binuclear complexes. In a study of the related $[(PPh_3)_2Cu(dpq)Cu(PPh_3)_2]^{2+}$ complex it was found that bridging ligand (BL) reduction occurred.[7] For that complex the reduction potential was ca. −0.9 V vs SCE. All of the binuclear complexes reported herein are much easier to reduce, the lowest reduction potential lying at −0.6 V vs SCE. Our results suggest that the dechelation versus BL reduction processes are balanced by electronic and structural factors.

Experimental Section

Synthesis. Ligands were prepared by the Schiff base condensation of a diamino compound with 2,2′-quinadil.[8] This was prepared in an analogous fashion to 2,2′-pyridyl from 2-quinoline carboxaldehyde.[9]

In a typical preparation 0.3 g (1×10^{-3} mol) of 2,2′-quinadil and 1 $\times 10^{-3}$ mol of the appropriate diaminobenzene were suspended in 100 mL of ethanol (freshly distilled from Mg/I_2)[10] and refluxed for 1 h. An orange-red color change was observed in the solution phase. After cooling, the solvent was removed under vacuum and the ligand was recrystallized from ethanol.

Mononuclear complexes were prepared by the rapid mixing of equimolar solutions ($CHCl_3$) of ligand and $[Cu(MeCN)_2(PPh_3)_2](BF_4)$. In a typical preparation 75.6 mg (1×10^{-4} mol) of $[Cu(MeCN)_2(PPh_3)_2](BF_4)$ was dissolved in $CHCl_3$ and made up to 100 mL in a volumetric flask. The same was done with 1×10^{-4} mol of the appropriate ligand. Rapid mixing resulted in a yellow-orange solution. The solvent was removed under vacuum and the complex was recrystallized from methanol.

Binuclear complexes were prepared by addition of 2 mol equiv of $[Cu(MeCN)_2(PPh_3)_2](BF_4)$ to 1 mol equiv of ligand in CH_2Cl_2. In a typical preparation 0.24 g (3.2×10^{-4} mol) of $[Cu(MeCN)_2(PPh_3)_2](BF_4)$ was added to a stirring solution of ligand (1.6×10^{-4} mol) in dichloromethane (20 mL). A rapid color change to dark red was observed. After 5 min of stirring the volume of the solution was reduced under vacuum and the complex was crystallized from the solution by slow ether diffusion.

2,3-(2′,2″)-Diquinolylquinoxaline (dqq). ^{1}H NMR ($CDCl_3$): δ 7.452 (m, 2H, 6′,6″); 7.500 (m, 2H, 7′, 7″); 7.561 (dd, J = 7.6, 1.6 Hz, 2H, 5′, 5″); 7.784 (dd, J = 7.4, 1.9 Hz, 2H, 8′, 8″); 7.848 (dd, J = 6.4, 3.4 Hz, 2H, 6, 7); 8.106 (d, J = 8.5 Hz, 2H, 3′, 3″); 8.226 (d, J = 8.5 Hz, 2H, 4′, 4″); 8.287 (dd, J = 6.5, 3.4 Hz, 2H, 5, 8). Anal. Calcd: C, 81.2; H, 4.2; N, 14.6. Found: C, 80.9; H, 3.9; N, 14.7. Yield 70%.

6,7-Dimethyl-2,3-(2′,2″)diquinolylquinoxaline (dqqMe$_2$). ^{1}H NMR ($CDCl_3$): δ 2.550 (s, 6H, $-CH_3$); 7.440 (m, 2H, 6′,6″); 7.492 (m, 2H, 7′, 7″); 7.557 (d, J = 7.7 Hz, 2H, 5′, 5″); 7.781 (dd, J = 7.4, 1.7 Hz, 2H, 8′, 8″); 8.029 (s, 2H, 5, 8); 8.071 (d, J = 8.6 Hz, 2H, 3′, 3″); 8.205 (d, J = 8.6 Hz, 2H, 4′, 4″). Anal. Calcd: C, 81.5; H, 4.9; N, 13.6. Found: C, 81.0; H, 4.9; N, 13.4. Yield 61%.

6,7-Dichloro-2,3-(2′,2″)diquinolylquinoxaline (dqqCl$_2$). ^{1}H NMR ($CDCl_3$): δ 7.508 (m, 6H, 5′, 5″, 6′, 6″, 7′, 7″); 7.810 (dd, J = 7.6, 1.7 Hz, 2H, 8′, 8″); 8.099 (d, J = 8.6 Hz, 2H, 3′, 3″); 8.265 (d, J = 8.6 Hz, 2H, 4′, 4″); 8.407 (s, 2H, 5, 8). Anal. Calcd: C, 68.9; H, 3.1; N, 12.4. Found: C, 68.7; H, 2.8; N, 12.3. Yield 75%.

$[(PPh_3)_2Cu(dqq)]BF_4$ (1·[BF$_4$]). Anal. Calcd: C, 70.3; H, 4.4; N, 5.3. Found: C, 70.3; H, 4.5; N, 5.5. Yield 30%.

$[(PPh_3)_2Cu(dqqMe_2)]BF_4$ (2·[BF$_4$]). Anal. Calcd: C, 70.1; H, 4.6; N, 5.2. Found: C, 70.3; H, 4.6; N, 4.9. Yield 25%.

$[(PPh_3)_2Cu(dqqCl_2)]BF_4$ (3·[BF$_4$]). Anal. Calcd: C, 66.0; H, 3.9; N, 5.0. Found: C, 66.0; H, 4.1; N, 5.1. Yield 56%.

$[(PPh_3)_2Cu(dqq)Cu(PPh_3)_2](BF_4)_2$ (4·[BF$_4$]$_2$). Anal. Calcd: C, 67.9; H, 4.4; N, 3.2. Found: C, 67.4; H, 4.1; N, 3.2. Yield 85%.

$[(PPh_3)_2Cu(dqqMe_2)Cu(PPh_3)_2](BF_4)_2$ (5·[BF$_4$]$_2$). Anal. Calcd: C, 67.5; H, 4.5; N, 3.2. Found: C, 67.7; H, 4.3; N, 3.0. Yield 85%.

$[(PPh_3)_2Cu(dqqCl_2)Cu(PPh_3)_2](BF_4)_2$ (6·[BF$_4$]$_2$). Anal. Calcd: C, 65.3; H, 4.1; N, 3.1. Found: C, 65.3; H, 4.6; N, 3.0. Yield 90%.

Physical Measurements. A Perkin-Elmer Lambda-19 spectrophotometer was used for collection of electronic absorption spectra. This was calibrated with a Ho_2O_3 filter and spectra were run with a 2 nm resolution.

For electrochemical and spectroscopic measurements solvents of spectroscopic grade were used. These were further purified by distillation and were stored over 5 Å molecular sieves. The supporting electrolytes used in the electrochemical measurements were tetrabutylammonium perchlorate (TBAP) and tetrabutylammonium hexafluorophosphate (TBAH). These were purified by repeated recrystallizations from ethanol/water for TBAP or ethyl acetate/ether for TBAH.[11]

Cyclic voltammograms (CVs) were obtained from argon-purged degassed solutions of compound (ca. 1 mM) with 0.1 M concentration of TBAP or TBAH present. The electrochemical cell consisted of a 1.6 mm diameter platinum working electrode embedded in a Kel-F cylinder with a platinum auxiliary electrode and a saturated potassium chloride calomel reference electrode. The potential of the cell was controlled by an EG&G PAR 273A potentiostat with model 270 software.

NMR spectra were recorded using a Varian 200 MHz NMR.

Raman scattering was generated using a Spectra-Physics model 166 argon ion laser. The sample was held in a spinning NMR tube or an optically transparent thin-layer electrode (OTTLE) cell, and the scattering was collected in a 135° backscattering geometry. The irradiated volume was imaged into a Spex 750M spectrograph using a two-lens arrangement.[12] The spectrograph was equipped with an 1800 g/mm holographic grating which provided a dispersion of 0.73 nm/mm. The Raman photons were detected using a Princeton Instruments liquid nitrogen cooled 1152-EUV charge-coupled detector controlled by a Princeton Instruments ST-130 controller. CSMA v2.4 software (Princeton Instruments) was used to control the CCD, and spectra were analyzed using GRAMS/32 (Galactic Industries Corp.) software. Spectral windows were approximately 18 nm wide and were calibrated using emission lines from a neon lamp or from an argon ion laser. The calibrations were checked by measuring the Raman band frequencies for known solvents.[13] It was found that, for the data reported herein, the calibrations were accurate to 1 cm^{-1}. Rayleigh and Mie scattering from the sample was attenuated using a Notch filter (Kaiser Optical Systems Inc.) of appropriate wavelength. A polarization scrambler was placed in front of the spectrograph entrance slit. A 150 μm slit width was used on the spectrograph, and this gave a resolution of approximately 6 cm^{-1} with 457.9 nm excitation.

The electronic absorption spectra of reduced species were measured using an OTTLE cell with a platinum grid as the working electrode.[14]

(6) Gordon, K. C.; McGarvey, J. J. *Inorg. Chem.* **1991**, *30*, 2986.
(7) Gordon, K. C.; Al-Obaidi, A. H. R. Jayaweera, P. M.; McGarvey, J. J.; Malone, J. F.; Bell, S. E. J. *J. Chem. Soc., Dalton Trans.* **1996**, 1591.
(8) Goodwin, H. A.; Lions, F. *J. Am. Chem. Soc.* **1959**, *81*, 6415.
(9) (a) Buehler, C. A.; Harris, J. O. *J. Am. Chem. Soc.* **1950**, *72*, 5015−5016. (b) Kaplin, H. *J. Am. Chem. Soc.* **1941**, *63*, 2654.
(10) Perrin, D. D.; Armarego, W. L. F.; Perrin, D. R. *Purification of Laboratory Chemicals*, 2nd ed.; Pergamon Press: Oxford, 1980; p 552.
(11) House, H. O.; Feng, E.; Peet, N. P. *J. Org. Chem.* **1971**, *36*, 2371.
(12) Strommen, D. P.; Nakamoto, K. *Laboratory Raman Spectroscopy*; John Wiley & Sons, Inc.: New York, 1984.
(13) Ferraro, J. R.; Nakamoto, K. *Introductory Raman Spectroscopy*; Academic Press Inc.: San Diego, CA, 1994.

Table 1. Crystal Data for **3**·[BF_4] and **6**·[BF_4]$_2$

identification code	**3**·[BF_4]	**6**·[BF_4]$_2$·2CH_2Cl_2
empirical formula	$C_{62}H_{44}BCl_2CuF_4N_4P_2$	$C_{51}H_{41}BCl_5CuF_4N_2P_2$
fw	1128.20	1071.40
temp, K	203(2)	293(2)
wavelength, Å	0.71073	0.71073
crystal system	triclinic	monoclinic
space group	$P\bar{1}$	$C2/c$
a, Å	10.956(2)	21.295(4)
b, Å	15.278(3)	24.322(5)
c, Å	16.032(3)	20.034(4)
α, (deg)	100.342(8)	90
β, (deg)	95.291(13)	112.64(3)
γ, (deg)	93.968(12)	90
V, Å^3	2618.6(9)	9576.8(3)
Z	2	8
ρ(calcd), (Mg/m)	1.431	1.486
μ, mm^{-1}	0.641	0.857
final R indices [$F > 4\sigma(F)$]	$R(F_o) = 0.0651$, $Rw(F_o^2) = 0.1590$[a]	$R(F_o) = 0.0422$, $Rw(F_o^2) = 0.1023$[a]

[a] $wR^2 = [([w(F_o^2 - F_c^2)^2]/([w(F_o^2)^2]]^{1/2}$ where $w^{-1} = [\sigma^2(F_o^2) + (aP)^2 + bP]$ for **3**·[BF_4] ($a = 0.0$; $b = 0.0$) and **6**·[BF_4]$_2$·2CH_2Cl_2 ($a = 0.0549$; $b = 35.0216$), $P = [\max(F_o^2,0) + 2F_c^2]/3$. The structure was refined of F_o^2 using all data; $R_1 = \sum||F_o| - |F_c||/\sum|F_o|$.

For Raman spectra of reduced species a similar cell was employed. Initial measurements found that the signal-to-noise of the Raman spectra were reduced because of reflection off the platinum grid. This problem was alleviated by removing a portion of the center of the grid (ca. 2 mm × 4 mm) and aligning the laser to irradiate the solution in that region.

Crystallography. Single crystals of **3**·[BF_4] were grown by the slow diffusion of diethyl ether into a solution of **3**·[BF_4] dissolved in dichloromethane. A yellow platelike crystal with approximate dimensions 0.15 × 0.25 × 0.20 mm^3 was selected and attached to the end of a glass fiber and cooled to −70 °C in a nitrogen stream. Crystallographic data are summarized in Table 1. Intensity data were collected using an Siemens SMART diffractometer (263 K, Mo Kα X-radiation, graphite monochromator, $\lambda = 0.710\,73$ Å). The data collection nominally covered over a hemisphere of reciprocal space, by a combination of three sets of exposures; each set had a different (angle for the crystal and each exposure covered 0.3° in ω. The crystal-to-detector distance was 4.94 cm. Coverage of the unique set is over 97% complete to at least 26° in θ. Crystal decay was monitored by repeating the initial frames at the end of data collection and analyzing the duplicate reflections, no decay was observed and no correction was applied. The data with index ranges $-13 \le h \le 13$, $-15 \le k \le 19$, $-20 \le l \le 18$ were employed for refinement. A total of 11 533 reflections were collected, of which 6749 were unique ($R_{int} = 0.1108$). The data were corrected for Lorentz, and polarization effects. Scattering factors are included in SHELX-93.[13] No correction for extinction was applied. The position of the Cu atom was determined from a Patterson synthesis. Calculations were carried out using a IBM-compatible computer and SHELX-93.[13] The remaining non-hydrogen atoms were located by application of a series alternating least-squares cycles and difference Fourier maps. All non-hydrogen atoms were refined with anisotropic displacement parameters. Hydrogen atoms were included in the structure factor calculations at idealized positions but were not subsequently refined. Final least-squares refinement of 685 parameters resulted in residuals, $R(F_o)$ of 0.0651 and $R_w(F_o^2)$ of 0.1590 [$F > 4\sigma(F)$] (4801 reflections). After convergence the quality-of-fit on F^2 was 0.964, and the highest peak in the final difference map was 0.603.

Single crystals of **6**·[BF_4]$_2$·2CH_2Cl_2, were grown by the slow diffusion of diethyl ether into a solution of **6**·[BF_4]$_2$ dissolved into dichloromethane. A red rod-shaped crystal with approximate dimensions 0.45 × 0.65 × 0.69 mm^3 was secured to the end of a glass fiber with cyanoacrylate glue. Crystallographic data are summarized in Table 1, and all other relevant data are available as Supporting Information. Intensity data were collected using an Enraf-Nonius CAD-4 diffractometer (293 K, Mo Kα X-radiation, graphite monochromator, (= 0.710 73 Å) in the range $3 \le 2\theta \le 40°$ by the ω scan motion with index ranges $0 \le h \le 19$, $0 \le k \le 23$, $-18 \le l \le 17$. A total of 4609 reflections were collected, of which 4450 were unique ($R_{int} = 0.0541$). The data were corrected for Lorentz, and polarization effects. No correction for extinction was applied. Scattering factors are included in SHELX-93.[15] Systematic monitoring of three check reflections showed no systematic crystal decay and no correction was applied. The position of the Cu atom was determined from a Patterson synthesis. Calculations were carried out using an IBM-compatible computer and SHELX-93.[1] The remaining non-hydrogen atoms were located by application of a series alternating least-squares cycles and difference Fourier maps. All non-hydrogen atoms were refined with anisotropic displacement parameters. Hydrogen atoms were included in the structure factor calculations at idealized positions but were not subsequently refined. Final least-squares refinement of 624 parameters resulted in residuals, $R(F_o)$ of 0.0422 and $R_w(F_o^2)$ of 0.1023 [$F_o > 4\sigma(F_o)$]. After convergence the quality-of-fit on F_o^2 was 0.978 and the highest peak in the final difference map was 0.420.

Table 2. Electrochemical Data for Reduction Waves of Ligands and Complexes in CH_2Cl_2 at Room Temperature (25 °C)[a]

compound	$E^{o\prime}$ vs SCE/V
dqq[b]	−1.71
$dqqMe_2$[b]	−1.75
$dqqCl_2$	−1.31
3	−0.80[c]
4	−0.53
5	−0.61
6	−0.32

[a] Reduction potentials are given versus SCE. Supporting electrolyte TBAP or TBAH. All waves are fully reversible, unless indicated, showing a ratio of currents for the anodic and cathodic peaks of unity and peak separation between anodic and cathodic waves of ca. 60 mV (ref 35). [b] Measured using DMF as solvent. [c] Does not show reversible electrochemistry.

Table 3. Electronic Absorption Data for Ligands and Complexes in CH_2Cl_2[a]

compound	λ/nm ($\epsilon \times 10^{-3}$/dm^3 mol^{-1} cm^{-1})			
dqq	255 (89)		334 (27)	
$dqqMe_2$	261 (87)		324 (26)	
$dqqCl_2$	260 (88)		349 (24)	
1	267 (82)	310[s] (25)	368 (16)	420[s] (3.3)
2	273 (54)	315[s] (19)	380 (14)	417[s] (3.9)
3	272 (83)	311[s] (26)	374 (19)	437 (3)
4	265 (83)	335 (27)	374[s] (20)	474 (4.8)
5	261 (86)	338 (29)	379[s] (22)	461 (5.3)
6	267 (88)	337 (25)	380[s] (19)	503 (3.7)

[a] Superscript "s" denotes shoulder.

Results

Electrochemistry. Electrochemical data for the ligands and complexes are shown in Table 2. The mononuclear complexes show irreversible reduction waves. The binuclear complexes have reversible reductions. The $E^{o\prime}$ values follow **6** > **4** > **5**. The ligand reductions lie in the same order, with the most electron deficient ligand, $dqqCl_2$, being the easiest to reduce and the electron rich $dqqMe_2$ the most difficult.

Electronic Spectra. The electronic spectral data for the ligands and complexes are presented in Table 3. The lowest transition for the ligands lies in the 320−330 nm region. This is assigned as a $\pi \rightarrow \pi^*$ transition. The energy of this transition is lowest for $dqqCl_2$ and highest for $dqqMe_2$. A further transition is observed at ca. 260 nm. No $n \rightarrow \pi^*$ transitions are seen for these ligands. Such transitions are generally weak.[16]

(14) Babaei, A.; Connor, P. A.; McQuillan, A. J.; Umapathy, S. *J. Chem. Educ.* **1997**, *74*, 1200.
(15) Sheldrick, G. M. *SHELXL-93−97*; Institut für Anorganische Chemie der Universität Göttingen: Germany, 1993.
(16) Badger, G. M.; Pettit, R. *J. Chem. Soc.* **1952**, 1874.

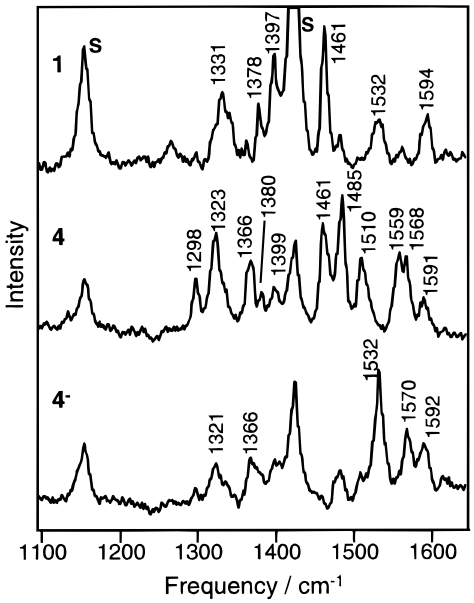

Figure 2. Resonance Raman spectra ($\lambda_{exc} = 488$ nm, 25 mW) of (upper trace) **1** (2 mM) in CH_2Cl_2; (middle trace) **4** (2 mM) in CH_2Cl_2; and (lower trace) $\mathbf{4}^-$ (2 mM) in CH_2Cl_2. Solvent bands are labeled S.

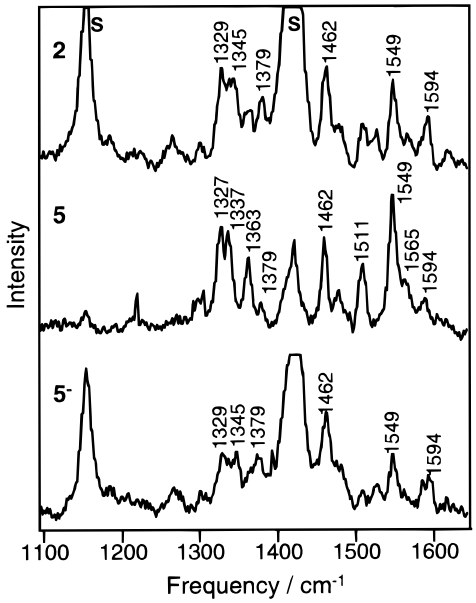

Figure 3. Resonance Raman spectra ($\lambda_{exc} = 488$ nm, 25 mW) of (upper trace) **2** (2 mM) in CH_2Cl_2; (middle trace) **5** (2 mM) in CH_2Cl_2; and (lower trace) $\mathbf{5}^-$ (2 mM) in CH_2Cl_2. Solvent bands are labeled S.

The mononuclear complexes show a long wavelength shoulder of moderate intensity ($\epsilon \sim 3000$ M^{-1} cm^{-1}). This is assigned as a metal-to-ligand charge-transfer (MLCT) transition. The energy of this transition follows the same pattern as that for the free ligands; **3** has the lowest energy. It is interesting to note that the ϵ drops as the transition energy decreases.

The binuclear complexes also show MLCT transitions as the lowest energy visible absorption. This is consistent with the more positive $E^{\circ\prime}$ values for reduction, which indicates that the presence of the second metal stabilizes the reduction. The reduction in (with lower transition energy for the MLCT band is also observed.

Resonance Raman Spectra. Resonance Raman spectra for the mononuclear complexes generated with 488 nm excitation are shown in Figures 2−4. These spectra are similar, all three complexes show bands at about 1594 and 1378 cm^{-1}. Other bands shift with substitution at the quinoxaline ring. The strongest band in **1** and **2** lies at 1460 cm^{-1}, this shifts to 1450 cm^{-1} in **3**. Also of note is a very intense band at ca. 1530 cm^{-1} in the spectrum of **1** and **3**.

All of the bands observed in the binuclear complexes are seen in the corresponding mononuclear spectra, with some small shifts in wavenumber values. However, the relative enhancements of the bands are quite different from mono- to binuclear complexes.

The resonance Raman spectra of the binuclear complexes show strong excitation wavelength dependence.[17] For **4** bands at 1323 and 1559 cm^{-1} are enhanced into the red with a band at 1510 cm^{-1} showing strongest enhancement with blue excitation. For **5** the 1549 cm^{-1} band shows strongest enhancement with 514.5 nm excitation. The 1511 cm^{-1} shows greater

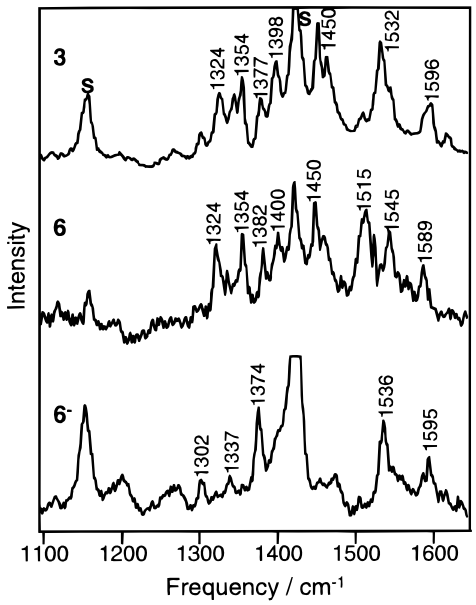

Figure 4. Resonance Raman spectra ($\lambda_{exc} = 488$ nm, 25 mW) of (upper trace) **3** (2 mM) in CH_2Cl_2; (middle trace) **6** (2 mM) in CH_2Cl_2; and (lower trace) $\mathbf{6}^-$ (2 mM) in CH_2Cl_2. Solvent bands are labeled S.

enhancement at 457 nm. For **6** the 1545, 1450, 1354, and 1324 cm^{-1} bands have increased enhancements out to 514.5 nm. The bands at 1515 and 1400 cm^{-1} show maximum enhancement at 457.9 nm. This strongly suggests that the broad absorption feature in the electronic spectrum of the complexes is made up of at least two transitions, the population of which results in different geometry changes on the bridging ligand. That is, the nature of the acceptor orbital of the BL or the donor MO of the metal is significantly different for the two transitions.

Spectroelectrochemistry. Changes in the electronic spectra of $dqqCl_2$ and **3** upon electrochemical reduction are shown in Figure 5.

For $dqqCl_2$ the reduction (Figure 5a) leads to the growth in of a band at 551 nm ($\epsilon \sim 2000$ M^{-1} cm^{-1}). The series of spectra measured at differing potentials across the reduction wave show

(17) The relative intensities of the complex bands may be parameterized by peak area ($I_{complex\ band}$) divided by the peak area of an internal standard band in the solution ($I_{solvent}$). In the case of solutions of **4**−**6** the solvent bands may act as the internal standard. The intensities of the complex and solvent bands were determined from the peak area corrected for baseline variations. The solvent band used was the 702 cm^{-1} peak as this is a strong feature and does not overlap with other solvent or complex bands. Some of the complex bands' enhancement factors could not be determined beause of overlapping features. Excitation profiles for **4**−**6** are provided in supporting material.

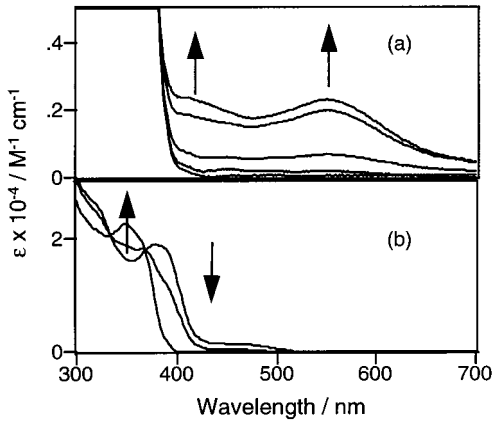

Figure 5. Changes in the electronic absorption spectrum of (a) $dqqCl_2$ (1mM) in CH_2Cl_2 as a function of applied potential, 0.0 to −1.6 V vs Ag wire, and (b) **3** (1 mM) in CH_2Cl_2 as a function of applied potential, 0.0 to −1.0 V vs Ag wire.

an isosbestic point at 381 nm. This suggests a single process is the dominant reaction probed in the OTTLE cell.

The reduction of **3** (Figure 5b) results in a bleaching of the MLCT band at 437 nm. The resultant spectrum is identical to that of the free ligand, $dqqCl_2$.

The binuclear complexes undergo electrochemical reduction. The absorption spectra (see Supporting Information for spectra) show depletion of the MLCT bands for the parent species with the reduced species absorbing to the blue. Isosbestic points are observed at 310 nm for **4** → **4**$^-$; 319 nm for **5** → **5**$^-$; 320 nm for **6** → **6**$^-$. For **5**$^-$ the observed spectrum is similar to that of the corresponding mononuclear complex, **2**. Furthermore, the spectral changes for **4** and **6** are fully reversible; those observed for **5** are not.

The resonance Raman spectra, generated with 488 nm excitation, of **4**−**6** and their reduced products are shown in Figures 2−4. Also shown are the resonance Raman spectra of the corresponding mononuclear species generated with 488 nm excitation.

Application of a reducing potential to the samples results in changes in the observed Raman spectra. The spectra of the reduced species contain no signal from the parent species. For **4** (Figure 2), reduction results in the depletion of the neutral species bands at 1559, 1510, and 1461 cm^{-1}. For **5** (Figure 3), bands at 1511 and 1363 cm^{-1} disappear upon reduction. For **6** (Figure 4), the intense neutral species bands at 1545, 1515, 1450, 1382, and 1354 cm^{-1} are all bleached upon reduction.

Discussion

Crystallography. The molecular structure of the cationic portion of **3** is shown in Figure 6. The ligand is quite large but no significant steric interactions are evident. The copper is held in a distorted tetrahedral environment with the Cu−P and Cu−N bond lengths being within the range reported for related complexes.[5,18] The P(1)−Cu−P(2) is 120.87(6)°, but the phosphine coordination is not symmetrical with respect to the mean Cu−N(1,2) plane. P(1) is slightly more axial, by 6°, than P(2). The only apparent reason for this distortion is the geometry of the ligand. The geometry of the ligand is interesting with the sections that are coordinating to the Cu(I) (the dichloroquinoxaline and one of the quinoline groups) being held in a slightly bent (15.5(3)° plane-to-plane) arrangement. This bending of the ligand is toward P(2) which appears to react by moving away to a more equatorial position. The structure in Figure 6 (right side) shows a view down the coordinating part of the ligand and the deviation of the free quinoline by 44.6(1)° from the mean plane of the rest of the ligand.

The molecular structure of **6**·$[BF_4]_2$·$2CH_2Cl_2$ is shown in Figure 7. The two sides of the molecule are related by symmetry operation (C2 rotation) and both coppers are therefore identical. In comparison to the structure of **3** the ligand has adopted a different geometry with significant deviations from planarity for the two sections of the ligand, the dichloroquinoxaline and the quinoline groups. The angle between the dichloroquinoxaline and the quinoline is 38.4(1)(and is probably due to unfavorable interactions between the protons on C3′ and C3″.[5] The copper is coordinated in a distorted tetrahedral geometry with a Cu−Cu′ distance at 6.892(9) Å. The bond lengths for the Cu−N and Cu−P bonds are all within the range reported for similar compounds.[15] The distortion of the geometry around the Cu atom is far more pronounced in **6** than was observed in **3**. The P(1)−Cu−P(2) angle is 124.30(8)° with P(1) being significantly more axial in nature that P(2). The angle between P(1) and the mean Cu−N(1,2) plane is 122.8-(1)°. In contrast, the angle between P(2) and the mean Cu−N(1,2) plane is 112.9(1)°. In this case the distortion is caused by an interaction between one of the phenyl rings on P(2) and the dichloroquinoxaline section of the ligand. The phenyl ring stacks above, and below, the pyrazine ring at an average distance of 3.536 Å, within range expected for π stacking.

As a result of the varying factors controlling the solid-state structures of **3** and **6** the ligand has quite different orientations. In **3** one of the quinoline lobes are effectively planar to the dichloroquinoxaline whereas in **6** neither of the two quinoline lobes is planar to the dichloroquinoxaline.

Electrochemistry and Electronic Spectra. The electrochemical data for the reduction potentials of the ligands show that the most electron deficient ligand is easiest to reduce. For the mononuclear systems there is no reversible reduction observed.

The presence of two copper(I) sites, as in the binuclear complexes, stabilizes the system to reduction. The $E^{\circ\prime}$ values show the same pattern as the ligands. This suggests the reduction in the binuclear complexes is occurring at the ligand or involves a redox orbital with significant ligand character.

The wavelength of the lowest energy electronic transition for **4**−**6** follow the reduction potential values. That is, the complex which is easiest to reduce, **6**, has the lowest energy transition, at 503 nm. A qualitative relationship between the $E^{\circ\prime}$ for reduction and the transition energy is indicative of an MLCT transition.[19]

As the λ_{max} for the MLCT band increases, the ϵ is observed to fall. McMillin *et al.*[20] examined the electronic spectroscopy of a series of copper(I) polypyridyl complexes. Using theories developed by Mulliken *et al.*[21] they demonstrated that the

(18) (a) Barron, P. F.; Dyason, J. C.; Engelhardt, L. M.; Healy, P. C.; White, A. H. *Aust. J. Chem.* **1985**, *38*, 261. (b) Engelhardt, L. M.; Pakawatchchai, C.; White, A. H.; Healy, L. M. *J. Chem. Soc., Dalton, Trans.* **1985**, 125. (c) Diez, J.; Gamasa, M. P.; Gimeno, J.; Tiripicchio, A.; Tiripicchio, C. *J. Chem. Soc., Dalton Trans.* **1987**, 1275. (d) Ainschough, E. W.; Baker, E. N.; Brader, M. L.; Brodie, M. L.; Ingham, S. L.; Waters, J. M.; Hanna, J. V.; Healy, P. C. *J. Chem. Soc., Dalton Trans.* **1991**, 1243. (e) Ainscough, E. W.; Brodie, A. M.; Ingham, S. L.; Waters, J. M. *J. Chem. Soc., Dalton Trans.* **1994**, 215.

(19) Juris, A.; Campagna, S.; Bidd, I.; Lehn, J.-M.; Ziessel, R. *Inorg. Chem.* **1988**, *27*, 4007.

(20) Phiffer, C. C.; McMillin, D. R. *Inorg. Chem.* **1986**, *25*, 1329.

(21) (a) Mulliken, R. S. *J. Am. Chem. Soc.* **1952**, *74*, 811. (b) Day, P.; Sanders, N. *J. Chem. Soc. A* **1967**, 1530. (c) Day, P.; Sanders, N. *J. Chem. Soc. A* **1967**, 1536.

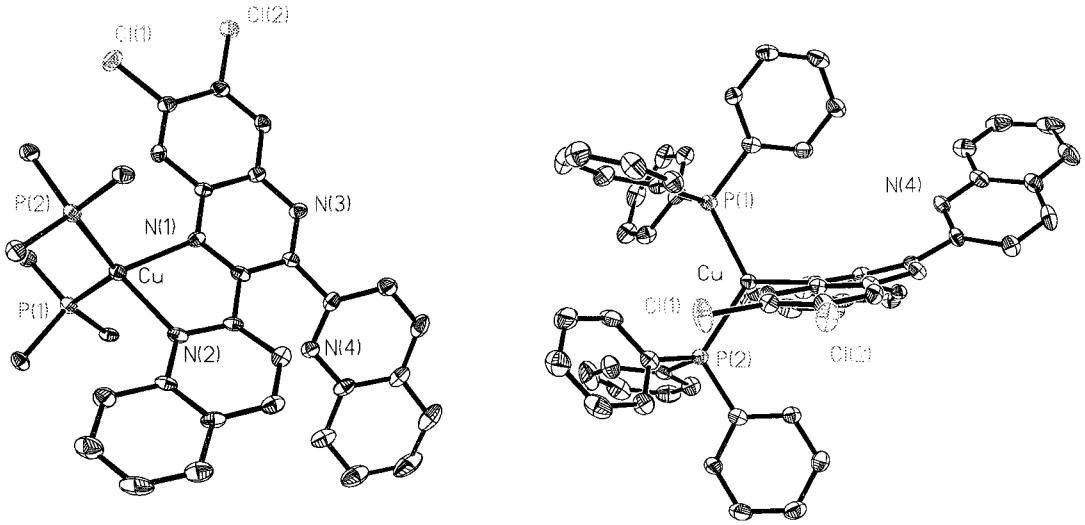

Figure 6. Molecular geometry of the cationic part of **3**·[BF_4]. For clarity part of the phenyl rings of the PPh_3 groups have been omitted from the left view. Ellipsoids are shown at the 50% probability level.

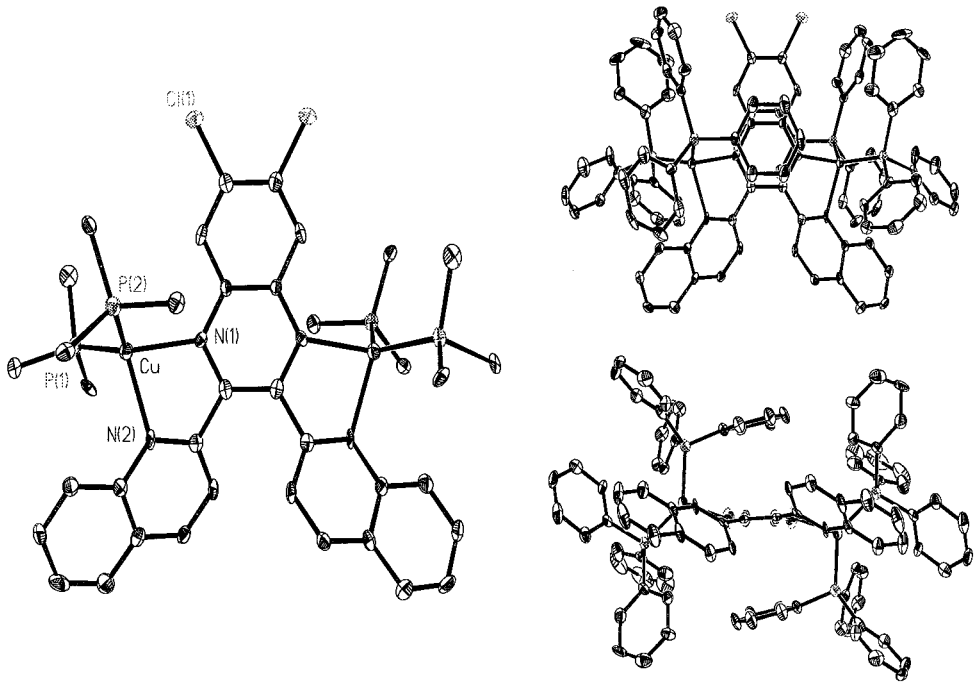

Figure 7. Molecular geometry of cationic part of **6**·[BF_4]·$2CH_2Cl_2$. For clarity, part of the phenyl rings of the PPh_3 groups has been omitted from the left view. The two right views have been reduced in size with respect to the left view, and the intramolecular π stacking is evident. Ellipsoids are shown at the 50% probability level.

transition intensity, as measured by ϵ, could be related to the dipole length of the transition. The distance between the acceptor orbital, BL π^* MO, and the donor site, the metal, is related to the intensity of the transition between the two orbitals. The greater the distance, the larger the ϵ value.

In terms of the binuclear complexes, in this study, there are two related phenomena which may be explained within the context of the Mulliken analysis. The transitions energies are reduced along with the ϵ, or dipole length. The dqq-based ligands used in this study possess two differing ring systems, each has two quinoline rings and a quinoxaline or substituted quinoxaline ring. The former are less electron deficient than the latter. Thus one might expect the acceptor orbital in an MLCT transition to have lower energy the greater its quinoxaline ring character. However, the greater the contribution of the quinoxaline ring to the acceptor MO the shorter the dipole length, by virtue of the fact that the quinoxaline is directly bound to the donor metal center. For the quinoline rings only one is bound to the donor metal site, the other being attached to the remote metal center. An acceptor MO with quinoline character will have a longer dipole length but a higher transition energy.

Clearly the actual nature of the of the donor and acceptor MOs is more complex than presented, nevertheless, this approach offers a qualitative insight into the nature of the MLCT transition. Furthermore, it is interesting to note the studies on the related dpq copper(I) systems reveal a similar pattern of behavior. The ϵ for **4**−**6** are greater than those reported for the corresponding dpq-based complexes of Yam.[22] This is consistent with the idea of dipole length being related to the distance between donor and acceptor orbitals. The larger quinoline rings provide extended distance for the π^* MO for BL from the metal center.

(22) Yam, V. W.; Lo, K. K. *J. Chem. Soc. Dalton Trans.* **1995**, 499.

Resonance Raman Spectra. The large number of atoms in these complexes, coupled with the low symmetry mean that there are many Raman active modes of vibration. All of the complexes show a large number of bands in the resonance Raman spectra in the 1000−1600 cm^{-1} region. A number of empirical points may be made about the form of the resonance Raman spectra:

(i) Each complex shows a distinct and unique spectral signature, this includes mono and binuclear complexes with the same BL and the mono- and binuclear series of compounds.

(ii) The frequencies of the observed bands are little shifted on going from mono- to binuclear complex, although the enhancement patterns are severely perturbed.

(iii) The observed spectra for the dqq based systems are significantly different from those of the related dpq complexes.

By comparing the spectra of related complexes it is possible to suggest assignments for the BL vibrations as being associated with either the quinoline or quinoxaline ring systems. The fact that the frequencies of the observed bands do not shift significantly on going from mono- to binuclear complex implies that the normal modes associated with the observed bands are BL in nature.

For $[Cu(dpq)(PPh_3)_2]^+$ and $Re(CO)_3Cl(dpq)$[23] the following bands are observed 1329, 1402, and 1471 cm^{-1} and 1325, 1360, and 1467 cm^{-1}. If these spectra are compared to that of **1**, two of the bands lie close in wavenumber to the dpq bands; these are at 1331 and 1397 cm^{-1}. In **1** a strong band is also present at 1461 cm^{-1}, shifted significantly from the 1471 observed in $[Cu(dpq)(PPh_3)_2]^+$. The 1330 and 1400 cm^{-1} bands appear to be associated with the quinoxaline, the 1460 cm^{-1} with the quinoline. Consistent with this assignment the quinoxaline bands shift with substitution. The spectrum of **2** shows bands at 1332 and 1346 cm^{-1}, there is no band at 1400 cm^{-1}, and the 1462 cm^{-1} is unshifted from **1**. On going to **3** the 1330 cm^{-1} region has bands at 1324, 1343, and 1354 cm^{-1}, a band is present at 1398 cm^{-1}, and a band at 1463 cm^{-1} is weak with a stronger band at 1450 cm^{-1}. The reduction in enhancement of the 1460 cm^{-1} band in **3** in comparison to **1** and **2** is consistent with the electronic absorption spectra which show that **3** has the lowest energy transition of the mononuclear complexes and the lowest ϵ. The reduced enhancement of a band associated with the quinoline ring suggests that the acceptor MO in the MLCT transition, the π^* bridging ligand orbital has greater quinoxaline character; the reduction in ϵ is consistent with this because the dipole length is shorter to the quinoxaline ring than the center of the two quinoline rings.

The spectra for binuclear complexes of the related dpq bridging ligand with ruthenium(II),[24] copper(I),[25] and rhenium(I)[26] are similar to one another. For $[(Cu(PPh_3)_2)_2(dpq)]^{2+}$ bands lie at 1286, 1319, 1364, 1471, 1493, 1566, and 1606 cm^{-1}. For the ruthenium(II) complex bands appear at 1273, 1308, 1357, 1461, 1488, 1562, and 1597 cm^{-1}. For the rhenium(I) complex bands are observed at 1293, 1321, 1366, 1467, 1497, 1558, and 1598 cm^{-1}. The SERS spectrum of quinoxaline shows a series of bands lying close in wavenumber to those reported above, for this reason the above bands are attributed to quinoxaline.[22] In **4** bands are observed at 1298, 1323, 1366, 1400, 1485, 1559, and 1591 cm^{-1} which show stronger enhancement on going to red excitation. Furthermore these bands are shifted on going to **5** and **6**, consistent with them being quinoxaline-based modes. In contrast, a number of bands appear common to **4**−**6** which do not appear in the spectra of $[(Cu(PPh_3)_2)_2(dpq)]^{2+}$ and $[Re(CO)_3Cl]_2(dpq)$ and show diminished enhancement with red excitation. These bands are weak in comparison to the quinoxaline-based modes. They lie at approximately 1335, 1380, 1510, and 1564 cm^{-1}. Some of these bands lie close in wavenumber to those of 2,2′-biquinoline (biq) as observed in $[Cu(biq)_2]^+$.[27] The biq modes lie at 1334, 1384, 1464, 1551, and 1601 cm^{-1}. Although, the similarities between the vibrational spectra of quinoline and quinoxaline make such distinctions difficult,[28] it appears correct to state that those bands that are strongly enhanced at 514.5 nm are similar to bands observed in complexes with dpq and shift with substitution at the quinoxaline ring. Most of the bands that show diminished enhancement at 514.5 nm are less sensitive to substitution at the quinoxaline ring and lie close to bands of $[Cu(biq)_2]^+$.

This suggests that, under the MLCT absorption band, there are two transitions: one terminating on a ligand MO with significant quinoxaline character and a second, at higher energy, terminating on a ligand MO with more quinoline character.

The 1510 cm^{-1} band is notable by its absence in spectra of dpq or biq. It is perhaps a delocalized mode coupling the two-ring systems. However, its relatively small shifting with quinoxaline substitution suggests significant quinoline character.

Spectroelectrochemistry. The reduction of $dqqCl_2$ (Figure 5a) results in increased absorption across the visible region. This is typical of radical anion species of polypyridyl ligands.[29]

Reduction of **3** (Figure 5b) does not result in ligand based radical anion formation. A bleaching of the MLCT band is observed as the parent species is reduced. The resulting spectrum is identical to that for the free ligand. This is consistent with the reduction occurring at the metal Cu(I) → Cu(0), which results in the dissociation of the complex. This behavior is common in copper(I) polypyridyl systems;[30] however, it is surprising that it occurs in a complex that is easily reduced and has an electron-deficient ligand. The clearest example of ligand-based reduction in copper(I) polypyridyl complexes occurs for $[Cu(dmbinap)_2]^+$ (dmbinap = 3,3′-dimethylene-2,2′-bi-1,8-naphthyridine).[31] Those complexes are considerably more difficult to reduce than **3**.

The reduction of the binuclear complexes (**4**−**6**) results in depletion of MLCT absorptions of the parent species. The reduced complexes do not correspond to the free-ligand spectra. For **5** → $\mathbf{5}^-$ the reduced species appears to possess an electronic absorption spectrum similar to **2**. For $\mathbf{4}^-$ and $\mathbf{6}^-$ the spectra do not correspond to the mononuclear complexes **1** and **3**. This suggests that **5**, which possesses an electron rich BL is separating into the mononuclear complex upon reduction.

$$\mathbf{5} + e^- \rightarrow \mathbf{2} + Cu + 2PPh_3$$

The resonance Raman spectrum of $\mathbf{5}^-$ confirms the formation of **2** as a reduction product. The resonance Raman spectra of $\mathbf{5}^-$ and **2** are identical (Figure 3).

(23) Waterland, M. W.; Simpson, T. J.; Gordon, K. C.; Burrell, A. K. *J. Chem. Soc. Dalton Trans.*, in press.
(24) Cooper, J. B.; MacQueen, D. B.; Petersen, J. D.; Wertz, D. W. *Inorg. Chem.* **1990**, *29*, 3701.
(25) Gordon, K. C.; McGarvey, J. J. *Chem. Phys. Lett.* **1990**, *173*, 443.
(26) Simpson, T. J.; Gordon, K. C. *Inorg. Chem.* **1995**, *34*, 6232.
(27) Leupin, P.; Schälphfer, C. W. *J. Chem. Soc., Dalton Trans.* **1983**, 1635.
(28) Carrano, J. T.; Wait, S. C., Jr. *J. Mol. Spectrosc.* **1973**, *46*, 401.
(29) Shida, T. *Electronic Absorption Spectra of Radical Ions*; Elsevier: Amsterdam, 1988.
(30) Masood, M. A.; Zacharias, P. S. *J. Chem. Soc., Dalton Trans.* **1991**, 111.
(31) Scott, S. M.; Gordon, K. C.; Burrell, A. K. *Inorg. Chem.* **1996**, *35*, 2452.

For **4** and **6** reduction does not result in the formation of the respective mononuclear complexes. The resonance Raman spectrum of $\mathbf{4}^-$ (Figure 2) shows a very strong band at 1532 cm^{-1} with weaker bands at 1570 and 1592 cm^{-1}. Although the 1532 cm^{-1} band is coincident with a band in the corresponding mononuclear complex, **1**, the strongest band for **1** at 1461 cm^{-1} is not present in $\mathbf{4}^-$.

A similar pattern is observed for $\mathbf{6}^-$. The most intense bands in the resonance Raman spectrum lie at 1374 and 1536 cm^{-1}. Both of these bands lie close to resonance Raman bands of **3** (1377 and 1532 cm^{-1}). However, the strongest features in the resonance Raman spectrum of **3** with 488 nm excitation lie at 1450 and 1398 cm^{-1}. These are absent in the spectrum of $\mathbf{6}^-$.

For **4** and **6** the reduction appears to be based on the bridging ligand. It is interesting to note that the electronic absorption spectrum of $dqqCl_2^-$ is unlike that of $\mathbf{6}^-$. This may be due to the differing geometries of these two species. Single-crystal X-ray studies of the related dpq ligand show it to have the pyridyl rings with the N pointed in to each other.[32] This is clearly not the configuration adopted by the ligand in **3** or **6**.

The resonance Raman spectra of $\mathbf{4}^-$ and $\mathbf{6}^-$ are similar but not identical. These spectra are unlike those of dpq and biq radical anion systems[24,33] suggesting the redox MO involves both quinoline and quinoxaline ring systems. Recently the resonance Raman spectra for a series of reduced dirhenium(I) complexes with dpq-based bridging ligand systems were reported.[24] In these complexes the spectra of the reduced species were identical. This finding was explained in terms of a localized redox molecular orbital in which the electron density was concentrated at the pyridyl ring systems for the differing ligands. The quinoline ring systems present in **4** and **6** also offer the possibility of electron localization; indeed the greater electron accepting ability of the quinoline over pyridyl ring may favor such a process. However, the spectral evidence suggests this has not occurred. There are a number of possible reasons for this:

(i) The two $[Cu(PPh_3)_2]^+$ units are insufficiently stabilizing to BL^-. For the binuclear $Re(CO)_3Cl$ systems it is known that the rhenium centers very strongly stabilize electron density suggesting the π^* MO of the ligand has a lot of metal character. The lesser stabilizing ability of the coppers may mean the electron acceptor MO has mostly ligand character. In that case stabilization of charge at the most electron deficient ring system would be anticipated.

(ii) The quinolines reduce the planarity of the ligand with respect to the three ring systems. This may reduce the ability of the two quinoline rings to stabilize the reducing electrons charge. This would lead to greater charge density for that electron at the quinoxaline ring system.

The suggestion that the redox MO is not strongly localized at the quinoline ring system is consistent with the electronic spectral data. The data may be interpreted in terms of the optical MO in **6** extending over the quinoxaline more than the quinoline rings.

The dissociation of $\mathbf{5}^-$ to **2** provides an insight into the factors the control stability of reduced species formed from copper(I) complexes.

Until recently, very few copper(I) polypyridyl complexes showed ligand-based reduction electrochemistry. Those that appear stable do so by having very electron-deficient ligands,[29] thus forming radical anion species, or by having ligands which encapsulate the reduced metal such that dechelation does not occur.[4] $[(Cu(PPh_3)_2)_2(dpq)]^{2+}$ forms a dpq-based radical anion species upon reduction. Yet it is significantly harder (0.3 V) to reduce than **5**. The ability to form a ligand-based radical anion species is not simply related to ease of reduction. The most probable reason for the instability of $\mathbf{5}^-$ is the steric bulk of the $dqqMe_2$ ligand. However, if the steric effect dominated the nature of the electrochemical products then both **4** and **6** would dissociate upon reduction. By considering electronic and steric factors together it is possible to provide an explanation consistent with our results.

In the case of **5** the methyl groups appear to cause the reducing electron to reside in an MO which is localized at the quinoline rings because of the electron donating methyl groups on the quinoxaline. Thus the reduced electron will form a redox MO with significant charge density on the quinoline and quinoxaline rings. Assuming the π^* ligand orbital occupied by the reducing electron is bonding with respect to the inter-ring linkage then reduction will lead to a flattening out of the ligand and dissociation of the complex. The observation of a flattening of ligands with reduction has been observed in 2,2′-bipyridine- and 4,4′-bipyridine-based systems.[34]

For **4** and **6** the reducing electron will reside over the quinoxaline ring, lowering the geometric distortions and resulting in less destabilization of the complex. This would occur more with the $dqqCl_2$ ligand than the dqq system. This is consistent with the different resonance Raman spectra for $\mathbf{4}^-$ and $\mathbf{6}^-$.

Conclusions

This work provides the first example of dechelation versus ligand based radical anion formation in the electrochemically reduced forms of a closely related group of complexes. Substitution effects on the quinoxaline ring system alter the nature of the acceptor MO or optical MO for the MLCT transition. They also appear to change the charge density distribution for the MO occupied by the reducing electron. It is clear that the use of such units in the construction of polynuclear copper(I) assemblies requires careful thought as both steric and electronic factors play a role in determining the outcome of reduction at one these units.

Acknowledgment. Support from the New Zealand Lottery Commission and the University of Otago Research Committee for the purchase of the Raman spectrometer is gratefully acknowledged. S.E.P. thanks the University of Otago for a postgraduate scholarship. This work was supported, in part, by the New Zealand Public Good Science Fund (Contract No. UOO-508). We are grateful for support of this work from the Massey University Research Fund. We thank Associate Professor C. E. F. Rickard (University of Auckland) for data collection on $\mathbf{3}\cdot[BF_4]$.

Supporting Information Available: Crystallographic data, resonance Raman spectra of **4**, **5**, and **6** at 457.9, 488, and 514.5 nm excitation, changes in the electronic absorption spectra of **4**, **5**, and **6** as a function of reducing potential, and resonance Raman spectra of **1**−**3** at 457.9 nm excitation are available (20 pages). Ordering information is given on any current masthead page.

IC9715052

(32) Richter, M. M.; Brewer, K. J. *Inorg. Chem.* **1990**, *29*, 3926.
(33) (a) Bungon, P.; Hester, R. E. *Chem. Phys. Lett.* **1983**, *102*, 537. (b) Al-Obaidi, A. H. R.; Gordon, K. C.; McGarvey, J. J.; Bell, S. E. J.; Grimshaw, J. *J. Phys. Chem.* **1993**, *97*, 10942. (c) Gordon, K. C.; McGarvey, J. J. *Chem. Phys. Lett.* **1989**, *162*, 117.
(34) (a) Danzer, G. D.; Golus, J. A.; Kincaid, J. R. *J. Am. Chem. Soc.* **1993**, *115*, 8643. (b) Schoonover, J. R.; Pingyun, C.; Bates, W. D.; Dyer, R. B.; Meyer, T. J. *Inorg. Chem.* **1994**, *33*, 793.
(35) Bard, A. J.; Faulkner, L. R. *Electrochemical Methods: Fundamentals and Applications;* Wiley: New York, 1980.